English summary of the thesis entitled

"Study of the stability and structure of the interaction of a free vortex with a flat surface perpendicular to its axis."

by L.Parras Anguita, directed by Ramón Fernández Feria.

1 Introduction

This thesis is devoted to study the interaction of a free vortex on a flat surface perpendicular to its axis. This vortex-plane interaction is interesting in industry due to the appearance of this proccess in vortex combustors and swirl atomizers. It is a problem of increasing interest because of its relation with atmospheric hazards like hurricanes and tornados. Related to the latter is the main interest of this thesis.

A tornado is defined by the National Weather Service (NWS) as "a violently rotating column of air in contact with the ground and extending from a thunderstorm base". A tornado does not necessarily have to be visible; however, the low pressures caused by the fast wind speeds usually cause water vapor in the air to condense into a visible condensation funnel. Tornados are one of the most destructive atmospheric hazards, because they usually have 180 km/h wind speeds, 75 m width and they can travel several kilometers, but they can reach up to 500 km/h windspeeds, core radius over 3 km and travel hudreds of kilometers. They are usually seen in the center states of USA, some parts of Canada, northwestern Europe and in central Asia and Africa plateaus. In Spain, they sometimes appear in the East coast (Levante).

The tornado lifecycle is a well known proccess. They appear when a big storm creates a mesocyclon, that is a swirling zone inside the storm (usually cyclonic, but it can also be anticyclonic). When the swirl is strong enough the tornado begins to move down until it reaches the ground forming what is known as Rear Flank Downwards (R.F.D.), that fix the point where the tornado touches the ground. In figure 1 is seen the proccess of reaching the ground where it is observed how the clouds move downwards. All this proccess is called *tornadogenesis* in the field of Meteorology. During the mature stage, the tornado increases the energy by pulling heat from the ground, the environment and the humidity of the air. In this stage, the R.F.D. has been putting in cold air from the storm, and this coldness starts to wrap it, cutting up the supply of hot air. This is the dissipation stage, in which it begins to slow down the swirling air that started the tornado, and then the tornado disappears, having the surface air more influence on it. This theory is generally accepted [see e.g. Edwards *et al.* (2005), Markowski (2002, 2003)] but it does not explain the genesis of some minor tornados as the *waterspouts* or *dustdevils*. However, it is clear that the physical mechanism of all them is the fall of a high swirling jet to

Figure 1: In this figure it is observed the genesis of a tornado. In the tree images sequence is shown how the funnel goes down until it reaches the ground. (Images taken from http://www.noaa.gov)

the ground. This is the reason of our interest in studying the interaction of a (simple model) vortex with the ground, to gain insight on how this interaction may produce such high vortices.

Actually, it is well known that flow in the eye of a tornado is slower than the surrounding air and usually directed downwards, as is seen in numerous experimental observations included in Ward (1972), Wan & Chang (1972) and Maxworthy (1982), among others. In fact, depending on the swirl intensity, different structures appear associated to different solutions of the equations of motion, as it will be briefly discussed in the following section. When the swirl intensity is low, the flow appears to be an effusing jet with a structure called "one cell" (see figure 2), where the axis velocity is always directed upwards. When the swirl velocity is increased, it can appear the so called vortex breakdown phenomenon, that consists on the appearance of a region of flow recirculation

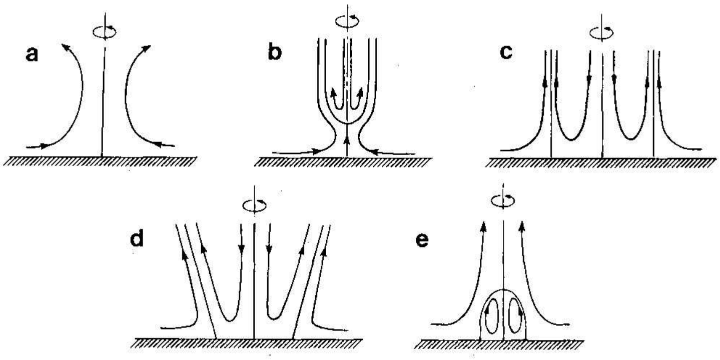

Figure 2: Different structures that can appear in the interaction of a free vortex with a flat surface, depending upon swirl intensity. In (a) it is presented a “one cell” solution. For moderate swirl intensity appears the so called “vortex breakdown”, (b), reaching a “two cell” solution in (c). In (d) are presented conical two cell solutions and in (e) solutions in which appear a “vortex ring” solution [Figure adapted from Lugt (1989)]

.

between two stagnation points at the axis, where the flow is directed downwards. If the swirl intensity is increased even more, the whole field near the axis is directed downwards, reaching the ground, creating a “two cell” structure.

In meteorological literature, during the last 50 years, many theories have arisen to explain the tornadogenesis via “vortex breakdown” phenomenon (Brandes, 1978, Wakimoto & Liu, 1998). There are some photographic evidences of the appearance of this phenomenon in real tornadoes. In Pauley & Snow (1988) a tornado is filmed in Minneapolis in which it is observed clearly the vortex core, and in it appears vortex breakdown at different stages of its development. On the other hand, the existence of different solutions of the equations for the same set of parameters make some authors state that the appearance of the tornado is related to the transition between solutions. It is in agreement with scarce experimental observations of high swirl tornados, that all of them have the double cell structure. However, not all high swirling flows interacting with a flat surface degenerate in a tornado, and the reason of this transition is obviously that the swirl intensity has to surpass a minimum critical value. One of the objectives of this work is to find that critical swirl intensity for a model of free vortex.

As it has been stated previously, this thesis pretends to improve the knowledge of the problem of the interaction of a vortex over a flat plate perpendicular to its axis, from a simple fluid mechanics point of view, without taking into account the thermodynamics of the real process. Several works in the field of meteorology have tried to study this phenomenon from the tornadogenesis point of view (Davies-Jones, 1982, Trapp, 1999), where it is studied the meteorological or dinamical conditions that are involved in the formation of a tornado, from a laboratory model (Ward, 1972) and from complex numerical simulations (Rotunno, 1978, Fiedler, 1995, Nolan & Farrell, 1998, Trapp, 1999, Lewellen *et al.* , 2000), where it is modelled a complex physics that include turbulence, ground roughness, downwards presure, air buoyancy, water vapor condensation, etc. The dinamical behavior of this phenomenon is often shadowed by this large set of parameters. Due to this fact, in this work, the simplest model has been chosen, with an axisymmetric and incompressible flow to obtain a problem that will be perfectly defined by the minimum set of parameters. The tornado is going to be modelled as a free vortex, because free vortex asymthotic solutions for high Reynolds numbers are avaliable.

1.1 Models of vortices interacting with a flat surface

In this last 50 years, several authors have dedicated part of their works to the problem of the interaction of a free vortex over a flat surface. One of the first was Taylor (1950), who studied the boundary layer solution of a potential vortex over a conical surface coaxial with it, related to the problem of the swirl atomizer. That kind of solutions can be characterized in cylindrical polar coordinates (r, θ, z) as (u, v, w)

$$(u, v, w) = \left(0, \frac{\Gamma}{r}, 0\right). \tag{1}$$

Afterwards, Rott & Lewellen (1966) searched for similarity solutions of the boundary layer generated by the interaction of the family of vortices

$$(u, v, w) = \left(0, \frac{\Gamma_n}{r^n}, 0\right), \tag{2}$$

with n ranging from -1 (solid rigid rotation) to 1 (potential vortex), that corresponds with (1). In that study, these researchers observed that the problem was reduced to a set of two ordinary differential equations, but these equations have solution only for some range of values of n ($-1 \leq n \leq 0.1$). In the case $n = -1$, the solution was the same as Bödewadt found 24 years before (Bödewadt, 1940). Later, the problem (2) was taken up again by Burggraf *et al.* (1971), and by Prahlad & Head (1976), that achieved to integrate the boundary layer equations over a finite disk. In particular, Burggraf *et al.* (1971) found a two layer similarity solution for the finite disk problem. This work was also considered by Belcher *et al.* (1972), who through numerical integration of the boundary layer equations over an infinite disk refined the range of n for which no slip solution existed $-1 \leq n \leq 0.1217$. Experimental evidences corroborate that the exponent n is different from $n = 1$ in flows of interest in real problems. In particular it can be seen in Ogawa (1993) and Gupta *et al.* (1984) that n can have values between 0.4 and 1 for confined and open flows (vortex chambers and tornados). That is the reason for the interest of vortex (2), which is more general than (1). However, both of them lack of meridional motion ($u = 0$, $w = 0$), which is not the case in flows of practical interest, in which the meridional flow is of the same order of magnitude as the swirl one. Therefore, it is necessary to take into account this meridional motion in order to study the interaction of a real vortex with a surface, even in the inviscid outer flow. A particular flow with meridional motion studied extensively in the literature is the family of vortices whose far from the axis field decrease inversely with the radius

$$\mathbf{u} = \mathbf{V}(y)\frac{1}{r}, \quad y = r/z, \tag{3}$$

where $\mathbf{V}(y)$ is a vectorial function whose three components can be obtained from the integration of two ordinary differential equations (see Sozou (1992) for more details). In fact, this is the only case in which the complete Navier-Stokes equations has a similarity solution. This family of solutions have been used as model of tornados (Serrin (1972), Shtern & Hussain (1993)), showing very interesting properties. Goldshtik (1960) and afterwards Serrin (1972), among others, demonstrated that it exists a critical value of Reynolds number above which this solution cannot satisfy the no slip boundary condition or the non singularity near the axis. In other words, there's a combination of parameters for which no similarity solution of the form (3) exist. This behavior was observed by Fernandez-Feria *et al.* (1999), in a more general family of solution of the form

$$\mathbf{u} = \mathbf{V}(y) r^{m-2}, \tag{4}$$

where $0 < m < 2$, that includes (3) for $m = 1$. However, for $m \neq 1$ the complete Navier-Stokes equations do not have similarity solutions of this form, but the Euler equations do. It is shown in Fernandez-Feria *et al.* (1999) that the solution can be obtained from the integration of an unique ordinary differential equation. This solution is singular at the axis ($y \to 0$) and on the wall ($y \to \infty$) for all the cases studied $0 < m < 2$. The regularization of the inviscid solution through a near axis boundary layer is only possible for a range of the swirl parameter, defined as

$$L = (v/w)_{y \to 0}. \tag{5}$$

That allowed range of values of L depends on m [see Fernandez-Feria *et al.* (1995)]. In particular, for $0 < m < 1$, the values of L have to be greater than a critical value, so there will not be solutions below this swirl intensity. The case $m = 1$ was studied for the first time by Long (1961), and only a value of swirl parameter is allowed ($L = \sqrt{2}$), and for this reason, meridional flow and swirling flow are always coupled in this case. This has been called the colapse phenomenon by Goldshtik (1960) for solutions of type (3). For $1 < m < 2$ it is shown that the allowed values of L are all below a critical value, and no solutions exist with higher swirl. Like it happens for vortices of type (3), the family of (inviscid) m-vortices (4) do not satisfy the no-slip boundary condition on the solid plane ($y \to \infty$). It was shown by Fernandez-Feria & Arrese (2000) that the viscous boundary layer equations governing the interaction of these vortices with the ground do not have self-similar solutions, in spite of the fact that the equations can be written in similarity form. However, a self-similar solution of the second kind was found, which will be used in this work as the boundary conditions for the numerical solution and the base flow for the stability analyses.

1.2 Objectives

The main objective of this work is to study the stability and structure of the interaction of a free vortex over a flat surface from an analytical, numerical and experimental point of view. To this end it has been solved the boundary layer solution of an m-vortex (Fernandez-Feria, 1995), over a flat surface, previously solved in Fernandez-Feria & Arrese (2000). It has been developed a formulation that eliminates the finite radius R_0 appearing in the similarity solution of the second kind for the boundary layer over the flat plate developed by Fernandez-Feria & Arrese (2000). We will use later this boundary layer solution as inflow of the numerical simulation. To know wether this solution is stable to non-axisymmetric perturbations for the design of an experiment it has been carried out an non-parallel local stability analysis of this similarity solution.

To solve the axisymmetric Navier-Stokes equation, it has been developed an steady state solver that use the pseudo-arclength method (Keller, 1977, Beran & Culick, 1992, Lopez *et al.* , 2001, Sanchez *et al.* , 2002) that can be used to study bifurcations in the flow. It has been characterized the particular case of the m-vortex which corresponds to Long's vortex (Long, 1961), that has been used extensively as a model of tornado, and for which $m = 1$. For this particular case, it has been proved that, for high Reynolds numbers, the solution reaches a similarity stage near the axis and far away the ground that can be compared with one of the two possible Long's solutions near the axis. In particular, our numerical solution tends to Type II solution, with flow directed downwards at the axis.

Finally, it has been designed and built an experimental setup to simulate this problem. The main aim of this experiment is to obtain the exponent m of a real vortex, and also to study the transitions between solutions and to characterize vortex breakdown.

2 Stability results

In this part it has been have studied the three dimensional, non parallel spatial stability of the boundary layer solution given in Fernandez-Feria & Arrese (2000). It has been developed the formulation for any value of m, but it has been solved numerically for the case of Long's vortex ($m = 1$ and $L = \sqrt{2}$), which is going to be the one simulated numerically. With this results we want to know whether or not the boundary layer solution, used as boundary condition in the axisymmetric simulation is stable. The other interest of this study is to provide information of the Reynolds numbers to design an experimental setup.

The main result of this section is the establishing of a formulation where the boundary layer and the non dimensional radius R are directly related. In the case of axisymmetric perturbations, for high Reynolds numbers (high radius), non viscous modes are the most unstable ones. When diminishing Reynolds number (see figure 3) the non viscous perturbations traveling to the center of the vortex decay and are finally damped. There also appears a new viscous mode that become more unstable than the non viscous one, decaying later and damping for a lower Reynolds than the non viscous one. Repeating this study for the rest of the azimuthal wave numbers it can be seen that all the threedimensional perturbations traveling to the center are damped for a critical Reynolds number of $R < 23$ as is shown in figure 4, where the region of stability is depicted for different Reynolds numbers.

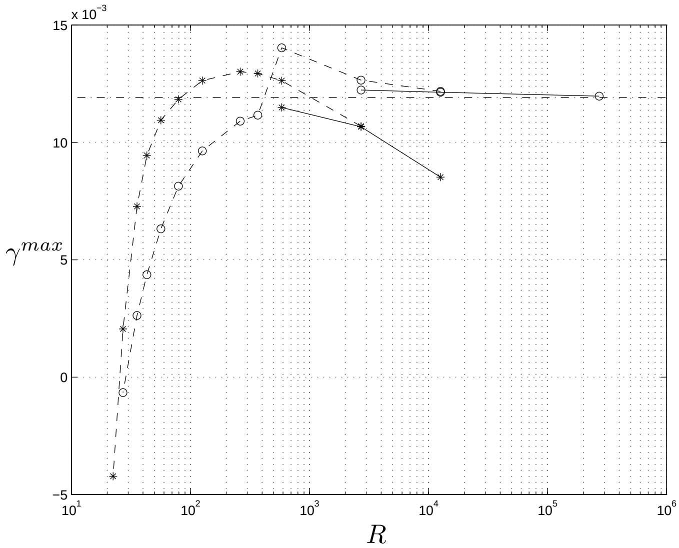

Figure 3: Maximum growth rate γ for each value of the Reynolds number (or radius) R. Viscous modes: (*). Inviscid modes: (o).

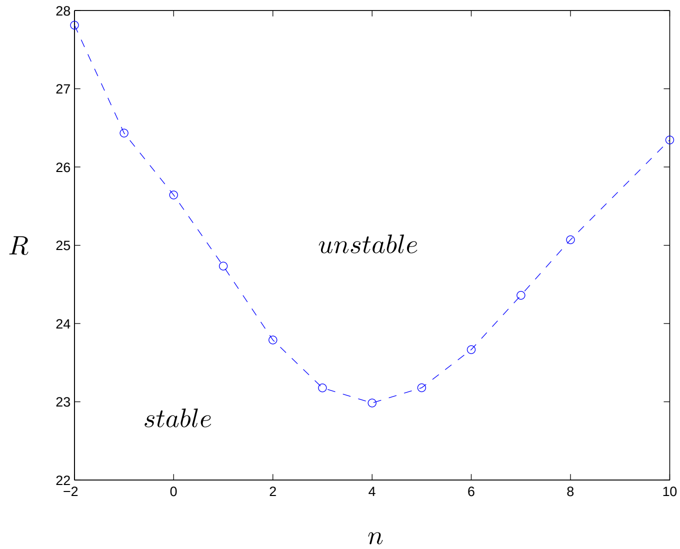

Figure 4: Region of instability in the plane (n, R), where n is the azimuthal wave number of the perturbations. It is observed that the critical Reynolds number is $R_c \simeq 23$, and the first instability as R increase corresponds to $n = +4$

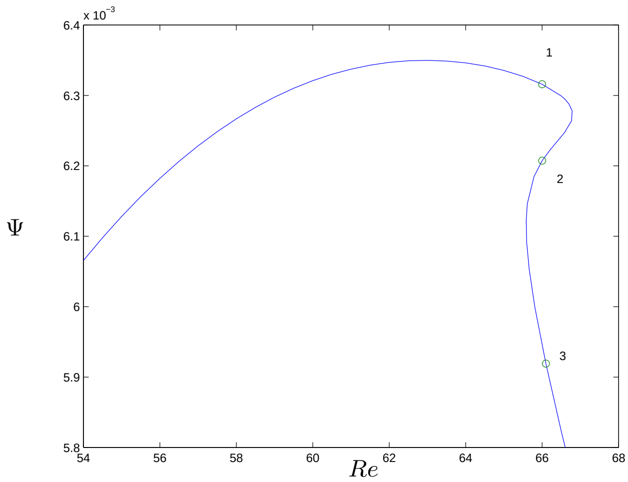

Figure 5: Example of limit point bifurcation. It is represented the value of the stream function in a fixed point near the recirculation bubble, as a function of Reynolds number. In this case, three solutions are possible for the same value of the Reynolds number. The solution 2 is unstable (see Lopez *et al.* (2001)). This can be seen as an hysteresis cycle.

3 Numerical Simulation

In this part we have developed an numerical code in FORTRAN that is able to solve the axisymmetric Navier-Stokes equations in cylindrical polar coordinates to obtain directly the steady state. This code is based in the work of Lopez *et al.* (2001) and Sanchez *et al.* (2002). It has been developed also a solver that allows to obtain the axisymmetric solution using a pseudo-arclength method [see Keller (1977), Beran & Culick (1992), Lopez *et al.* (2001), Sanchez *et al.* (2002)], which is able to detect bifurcation points. For instance, the solver is able to detect limit points, in which for a given value of Re the equations have tree possible solutions (see figure 5).

One of the contributions of this thesis is the formulation of the numerical simulation using as boundary conditions the asymthotic matching of the boundary layer solution with the outer solution. With this formulation, the problem is solved with a really free vortex boundary conditions. Figure 6 shows the boundary layer solution for the stream function together with the inviscid outer solution and the composite solution, which is the summation of the outer solution plus the boundary layer solution minus the common part of the solution

With these two solvers we have analyzed the problem of the interaction of Long's vortex over a flat surface. For this case it has been solved the problem until very high Reynolds number, for which it has been obtained a similarity solution behavior far away from the ground and near the axis. These solutions have been compared with previous results on the similarity solutions of Long's vortex near the axis (Long, 1961, Burggraf & Foster, 1977, Fernandez-Feria *et al.* , 1995). The more interesting result is that two possible solutions of the near

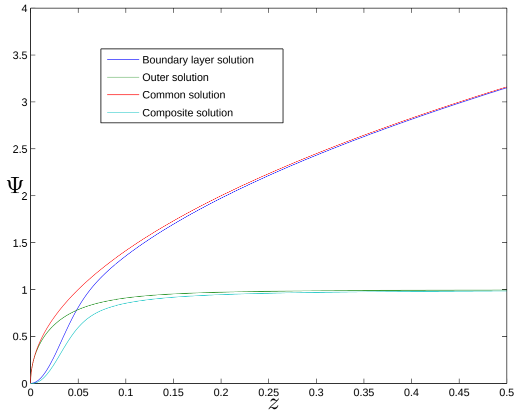

Figure 6: In this figure is presented an example of matching the external solution with the boundary layer solution for $Re = 10$.

axis boundary layer equations exist at high Reynolds numbers. These are the so called type I or type II solutions by Burggraf & Foster (1977), depending on whether it has a maximum or a minimum in the axial velocity at the axis. The interaction of this vortex with a flat surface selects just one of them, which is found have to be the type II solution with negative velocity at the axis. And what is even more interesting, it selects the asymptotic minimum value of the axial velocity in the axis.

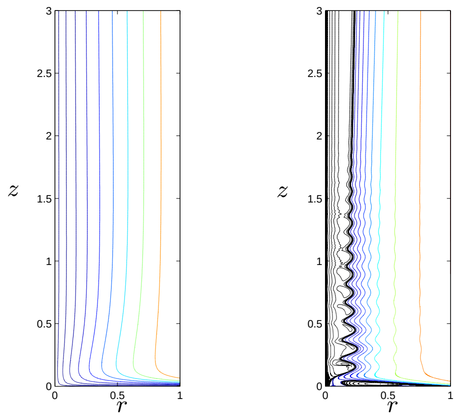

Figure 7: This figure present two example of solutions obtained. The stream function is presented for two different Reynolds number. The one in the left corresponds to a low Reynolds number ("one cell" solution) and the one on the right for a high Reynolds number, in which in black is presented reversed flow ("two cell").

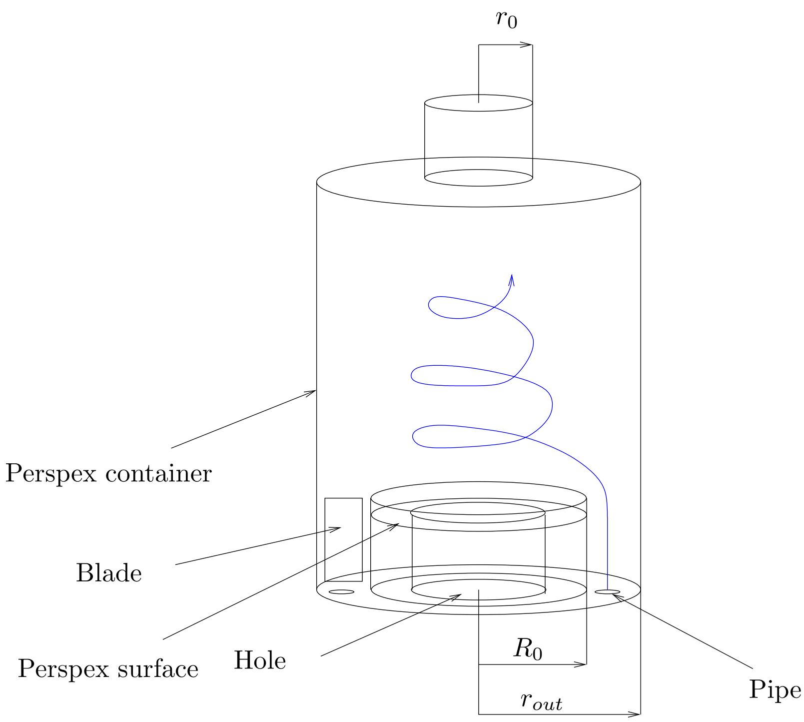

Figure 8: Sketch of the experimental setup with some characteristic lengths. The flow enters through eight equally spaced pipes and turns due to the rotating blades.

4 Experimental Results

An experimental setup has been designed and built to simulate the problem of the interaction of a vortex over a solid surface. The design has been done basing our calculation on the stability results obtained before. Once this experimental setup has been built, we have measured the velocity field using a stereo PIV equipment. In this preliminary experimental work, we have just validated the design of the experiment and determined the exponent m of the radial decay of the azimuthal velocity.

Figure 8 shows a sketch of the experiment with the most important length scales. The flow enters the axisymmetric container through eight equally spaced pipes and is rotated through 36 blades connected to an AC motor. The flow rate, the angular velocity of the rotation and the temperature are monitorized through a program in Labview during each test. Flow rate has oscillations of less than a 1% and the angular velocity less than 2%. Two Reynolds numbers, one related the flow-rate and the other one based on the swirl velocity, are defined:

$$Re_Q = \frac{Q}{\pi r_0 \nu}, \quad Re_L = \frac{\Omega r_0^2}{\nu}. \tag{6}$$

Two measurement configurations have been studied, which are presented in figure 9. The first one (top) corresponds to the measurement of the 2D velocity

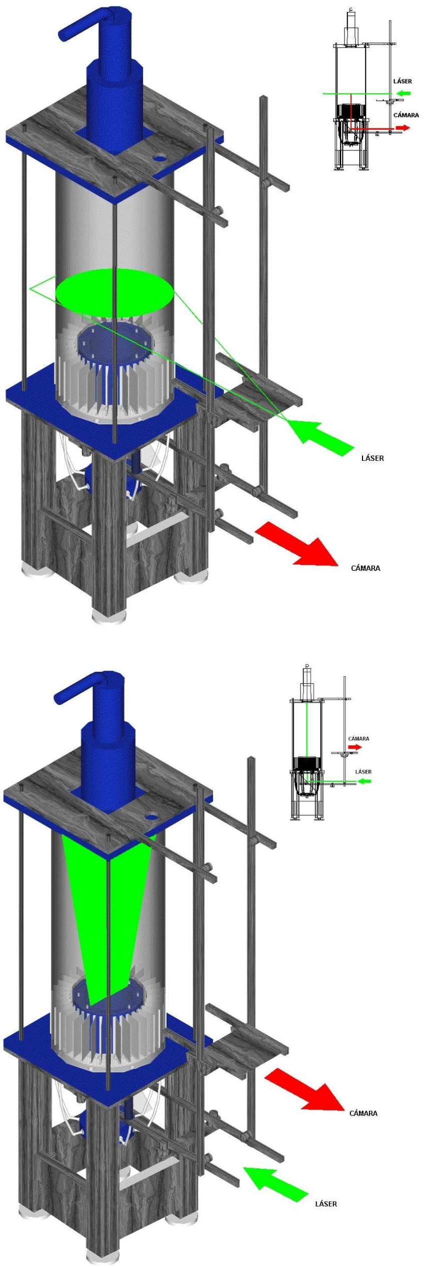

Figure 9: Pictures of the experimental setup with the two configuration studied. On the top, the two dimensional configuration, in which the laser is illuminates from the front side, and the camera takes the images through the surface of perspex by mean of a mirror. On the bottom, the stereo configuration, in which the laser illuminates through the surface of interaction and the images are taken with two cameras localized in front of the experiment.

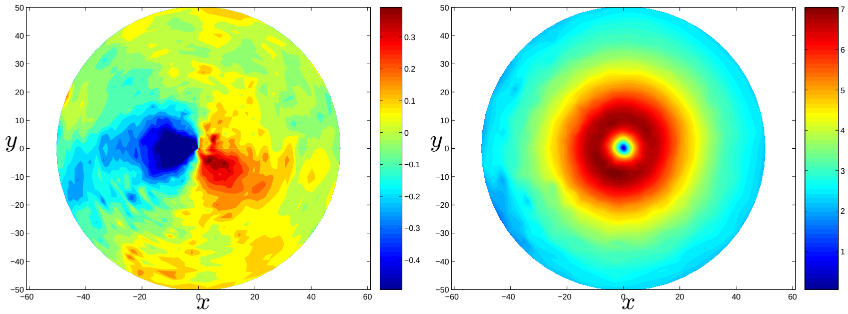

Figure 10: Velocity field obtained by 2D-PIV for $Re_Q = 1648.6$ and $Re_L = 570.5$. On the left it is shown the radial velocity and on the right the azimuthal velocity. Lengths dimensions are in mm and velocities are in cm/s.

field on a horizontal plane, and the second one (bottom) to a 3D measurement (with two cameras) of the velocity field on a vertical plane. The main interest of this study is to verify if the experiment fits our needs and to obtain an approximation of the value of the exponent m. For the two dimensional results, some fields have been obtained for different heights. An example is shown in figure 10 where the 2D field is represented in cylindrical polar coordinates.

The three dimensional results configuration have shown the existence of a neutral curve in the plane (Re_Q, Re_L) below which no swirl appears (see figure 11). In figure 12 axial and azimuthal velocities in a plane perpendicular to the

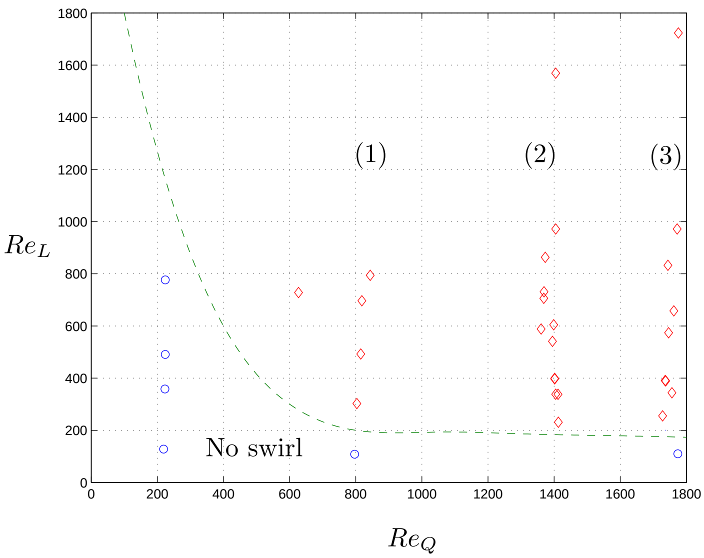

Figure 11: Summary of the 3D experimental measurements for different values of Re_Q and Re_L. In dashed lines it is presented the approximated transition between solutions with no swirl and with swirl. With (1), (2) and (3) are marked the three flow rates studied.

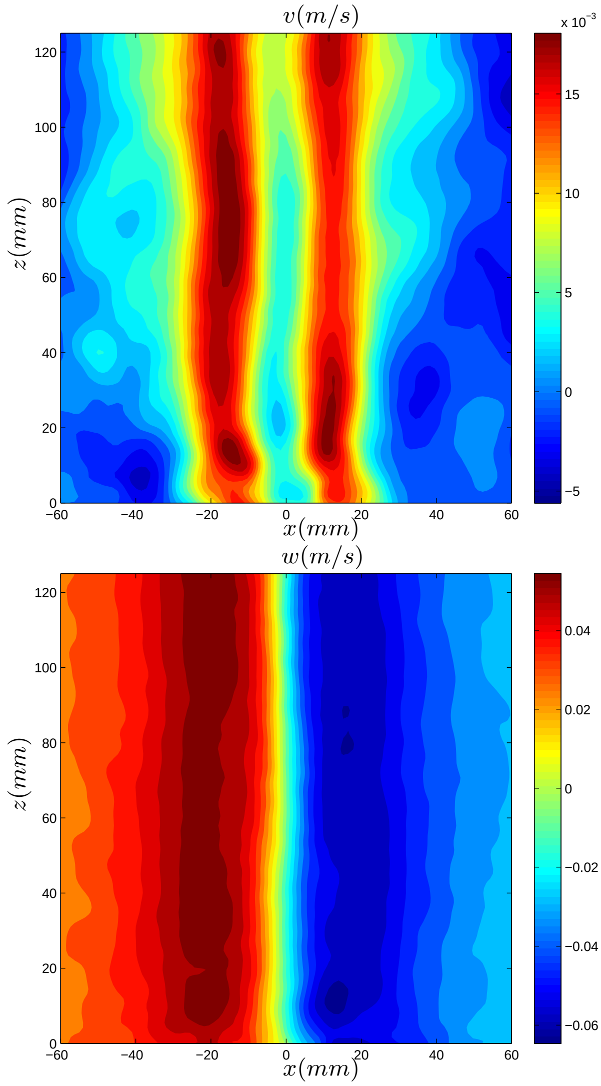

Figure 12: Velocity field in the vertical plane (r, z) obtained by stereoscopic PIV for $Re_Q = 1403.6$ and $Re_L = 234.1$. Top: Axial velocity. Bottom: Azimuthal velocity.

flat surface are shown, localized just in the geometric center of the experiment. A depression in axial velocity is located near the axis, due to the intensity of swirl, and an almost columnar vortex is formed. To determine the m coefficient, the solutions far away the ground have been used. Figure 13 shows an example of the radial profiles of the velocity field and of its fitting to a radial decay of the form r^{m-2}.

Repeating this proccess for all the Re_Q and Re_L cases studied, we have obtained that the decaying coefficient is not dependent on each of the parameters separately, but on a relation between them. In particular, we find that m depends only on the swirl parameter $L_{exp} = Re_L/Re_Q$, and that this dependence

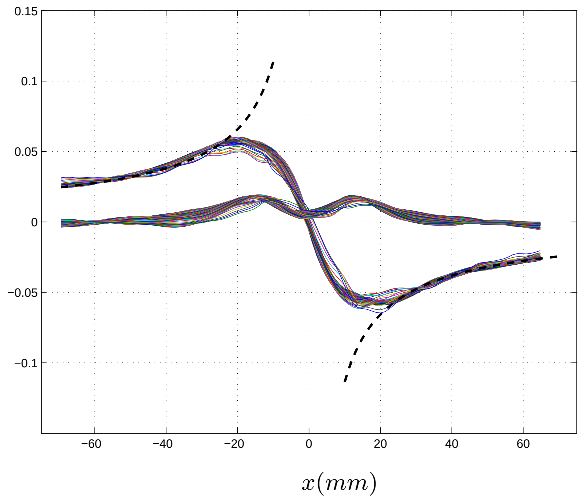

Figure 13: Azimuthal and axial velocities as a function of the radial coordinate ($r = x$, for $x \gg 0$) for the upper half of the axial and azimuthal profiles corresponding to figure 12. In dashed lines is presented the adjustment of the azimuthal velocity, for which an exponent of $m = 1.2 \pm 0.07$ has been obtained.

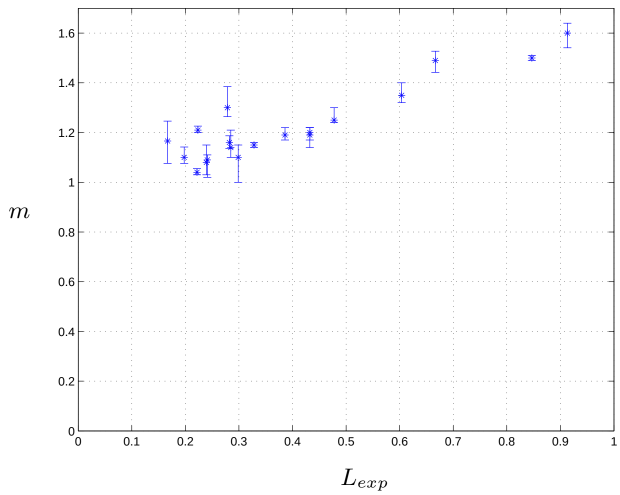

Figure 14: This figure shows all the cases studied that are not unstable, and for which we have obtained the value of m. It is seen the linear dependence on the experimental swirl parameter L_{exp}.

is almost linear (see figure 14).

Bibliography

Belcher, R.J., Burggraff, O.R., & Stewartson, K. 1972. On generalized-vortex boundary layers. *J. Fluid. Mech.*, **52**, 753–780.

Beran, P.S., & Culick, F.E.C. 1992. The role of non-uniqueness in the development of vortex breakdown in tubes. *J. Fluid Mech.*, **242**, 491.

Brandes, E.A. 1978. Mesocyclone evolution and tornadogenesis: Some observations. *Mon. Wea. Rev.*, **106**, 995–1011.

Burggraf, O.R., & Foster, M.R. 1977. Continuation or breakdown in tornado-like vortices. *J. Fluid. Mech.*, **80**, 685–703.

Burggraf, O.R., Stewartson, K., & Belcher, R.J. 1971. Boundary Layer Induced by a Potential Vortex. *Phys. Fluids*, **14**, 157–169.

Bödewadt, U.T. 1940. Die Drehstromunguber festem Grunde. *ZAMM*, **20**, 251.

Davies-Jones, R. P. 1982. Observational and Theoretical Aspects of Tornadogenesis. *In:* L., Bengtsson, & J., Lighthill (eds), *Intense Atmospheric Vortices.* Springer-Verlag, Berlin Heidelberg (Germany).

Edwards, Moller, & Purpura. 2005. *Basic Spotters' Field Guide.* Tech. rept. U.S. Department of Commerce. National Oceanic and Atmospheric Administration.

Fernandez-Feria, R. 1995. Viscous and inviscid instabilities of non-parallel self-similar axisymmetric cores. *J. Fluid. Mech.*, **305**, 77–91.

Fernandez-Feria, R., & Arrese, J.C. 2000. Boundary layer induced by a conical vortex. *Q. Jl Mech. appl. Math*, **53**(4), 609–628.

Fernandez-Feria, R., Fernandez de la Mora, J., & Barrero, A. 1995. Solution breakdown in a family of self-similar nearly inviscid axisymetric cores. *J. Fluid. Mech.*, **305**, 77–91.

Fernandez-Feria, R., Fernandez de la Mora, J., Perez-Saborid, M., & Barrero, A. 1999. Conically similar swirling flows at high Reynolds numbers. *Q. Jl Mech. appl. Math*, **52**, 1–53.

Fiedler, B.H. 1995. On Modelling Tornadoes in Isolation from the Parent Storm. *Atmos. Ocean*, **33**, 501–512.

Goldshtik, M. A. 1960. On swirling jets. *Appl. Mat. Mech.*, **24**, 610–621.

Gupta, A.K., Lilley, D.G., & Zang, T.A. 1984. *Swirls Flows.* Abacus Press.

Keller, H.B. 1977. Numerical solution of bifurcation and nonlinear Eigenvalue problems. *In:* Rabinowitz, A. (ed), *Applications of Bifurcation Theory.* Academic, 1977.

Lewellen, D.C., Lewellen, W.S., & Xia, J. 2000. The Influence of a Local Swirl Ratio on Tornado Intensification near the Surface. *J. Atmos. Sci.*, **57**, 527–544.

Long, R.R. 1961. A vortex in an infinity viscous fluid. *J. Fluid Mech.*, **11**, 611–625.

Lopez, J.M., Marques, F., & Sanchez, J. 2001. Oscillatory modes in an enclosed swirling flow. *J. Fluid. Mech.*, **439**, 109–129.

Lugt, H. J. 1989. Vortex breakdown in atmospheric columnar vortices. *Bull. Amer. Meteor. Soc.*, **70**, 1526–1537.

Markowski, P. 2002. Hook Echoes and Rear-Flank Downdrafts: A Review. *Monthly Weather Review*, **130**, 852–876.

Markowski, P. 2003. Tornadogenesis Resulting from the Transport of Circulation by a Downdraft: Idealized Numerical Simulations. *Jou. Atmos. Sci*, **60**, 795–823.

Maxworthy, T. 1982. The Laboratory Modelling of Atmospheric Vortice: A Critical Review. *In:* Bengtsson, L., & Lighthill, J. (eds), *Intense Atmospheric Vortices*. Springer-Verlag, Berlin Heidelberg (Germany).

Nolan, D.S., & Farrell, B.F. 1998. The Structure and Dynamics of Tornado-Like Vortices. *Jou. Atmos. Sci.*, **56**, 2908–2936.

Ogawa, A. 1993. *Vortex Flows*. CRC Press, London.

Pauley, R. L., & Snow, J. T. 1988. On the kinematics and dynamics of the 18 Julay 1986 Mineapolis tornado. *Mon. Wea. Rev.*, **116**, 2731–2736.

Prahlad, T.S., & Head, M.R. 1976. Numerical solutions for boundary layers beneath a potential vortex. *Computers and Fluids*, **4**, 157–169.

Rott, N., & Lewellen, W.S. 1966. Boundary Layers and their interactions in rotating flows. *In:* Kucheman, E. (ed), *Progress in Aeronautical Science*, vol. 7. Pergamon, NY, 1966.

Rotunno, R. 1978. A Study in Tornado-Like Vortex Dynamics. *J. Atmos. Sci.*, **36**, 140–155.

Sanchez, J., Marques, F., & Lopez, J.M. 2002. A continuation and bifurcation technique for Navier-Stokes flows. *J. Comput. Phys*, **180**, 78–98.

Serrin, J. 1972. The Swirling Vortex. *Phil. Trans. R. Soc. A*, **271**, 327–380.

Shtern, V., & Hussain, F. 1993. Hysteresis in a swirling jet as a model of tornado. *Phys. Fluids A*, **5**, 2183–2195.

Sozou, C. 1992. On solutions relating to conical vortices over a plane wall. *J. Fluid. Mech.*, **244**, 633–644.

Taylor, G.I. 1950. The boundary Layer in the converging nozzle of a swirl atomizer. *Q. Jl. Mech. appl. Math.*, **3**, 129–139.

Trapp, J. 1999. A Clarification of Vortex Breakdown and Tornadogenesis. *Mon. Wea. Rev.*, **128**, 888–895.

Wakimoto, R.M., & Liu, C. 1998. The Garden City, Kansas, storm during VORTEX 95. Part II: The wall cloud and tornado. *Mon. Wea. Rev.*, **126**, 393–408.

Wan, C.A., & Chang, C.C. 1972. Measurements of the velocity fields in a simulated tornado-like vortex using a three dimensional probe. *Jou. Atmos. Sci.*, **29**, 116–127.

Ward, N.B. 1972. The explanation of certain features of tornado dynamics using a laboratory model. *J. Atmos. Sci.*, **29**, 1194.